Accelerating Non Linear Perfect Foresight Model Solution by Exploiting the Steady State Linearization

Gary S. Anderson
Board of Governors
Federal Reserve System
Washington, DC 20551*
Voice: 202 452 2687
Fax: 202 452 6496
ganderson@frb.gov

JEL classification: C63–Computational Techniques†

September 1, 1998

Abstract

Linearizing non linear models about their steady state makes it possible to use the Anderson-Moore Algorithm(AIM) to investigate their saddle point properties and to efficiently compute their solutions. Using AIM to check the long run dynamics of non linear models avoids many of the burdensome computations associated with alternative methods for verifying the

*I wish to thank Vi-Min Choong, Brian Madigan, Jeffrey Fuhrer, and Volker Wieland for their helpful comments. I am responsible for any remaining errors. The views expressed herein are mine and do not necessarily represent the views of the Board of Governors of the Federal Reserve System.

†Subfields Applied Econometrics, Applied Macroeconomics, Other Topics in Mathematical Economics

saddle point property. In addition, for models that have the saddle point property, AIM provides a set of terminal conditions for solving the non linear model that work better than the traditional approach of setting the end of the trajectory to the steady state values. Furthermore, the asymptotic linear constraints can also generate initial conditions for the solution path that are better than initializing the solution path to the steady state values. Using the improved asymptotic constraints typically halves the computational burden associated with solving the nonlinear problem.

1 A Non-Linear Extension of the Anderson-Moore Technique

1.1 General Model Specification

Consider the model

$$h(x_{t-\tau}, x_{t-\tau+1}, ..., x_{t+\theta-1}, x_{t+\theta}) = 0 \quad (1)$$
$$t = 0, \ldots, \infty$$

Where $x \in \Re^L \; and \; h : \Re^{L(\tau+1+\theta)} \rightarrow \Re^L$. We want to determine the solutions to Equation 1 with initial conditions

$$x_i = \bar{x}_i \; for \; i = -\tau, ..., -1 \quad (2)$$

satisfying

$$\lim_{t\rightarrow\infty} x_t = x^*. \quad (3)$$

This paper shows how to adapt the methods of (Anderson & Moore, 1985) to determine the existence, and local uniqueness of the solution to Equation 1.

1.2 Asymptotic Linearization

If h were linear, we could immediately apply the methods of (Anderson & Moore, 1985) to determine the existence and uniqueness

of a perfect foresight solution and to compute the solution. Since h is non-linear, we will compute approximate solutions to system system 1 by using the nonlinear h constraints in Equation 1 for the initial part of the trajectory, and using a system of linear constraints which reflect the asymptotic properties of the system for the remainder of the trajectory.

This technique can be thought of as a generalization of the approach used by Fair-Taylor(Fair & Taylor, 1983). This paper describes a procedure which, unlike the Fair-Taylor approach, allows the solution to lie in the *stable subspace* of a linear system characterizing the asymptotic properties of the nonlinear system.

The steady state value x^* satisfies

$$h(x^*, ..., x^*) = 0 \tag{4}$$

Near the steady state, the linear first-order Taylor expansion of h about x^* provides a good approximation to the function h.

$$h(x_{t-\tau}, ..., x_{t+\theta}) \approx \sum_{i=-\tau}^{\theta} H_i|_{x^*} (x_{t+i} - x^*) \tag{5}$$

The technique presented in (Anderson & Moore, 1985) can determine the existence and uniqueness of perfect foresight solutions near the steady state of linear models. The asymptotic analysis of the linear model determines convergence properties before burdensome calculations of the nonlinear solutions. That stability analysis produces a matrix, Q, which restricts values of the endogenous variables to the stable subspace of the linearized system.

For trajectories which approach a steady state, one can ultimately replace the non-linear system with the constraints codified in the matrix Q.

$$Q \begin{bmatrix} x_{T-\tau} - x^* \\ \vdots \\ x_T - x^* \\ \vdots \\ x_{T+\theta} - x^* \end{bmatrix} = 0 \tag{6}$$

Consequently, for solutions which converge to the steady state, we can, in principal, compute solutions to whatever accuracy required by increasing the magnitude of T.

1.3 Relationship to Traditional Approach Using Fixed Points

The more traditional Fair-Taylor approach also increases T to increase accuracy, but it imposes Equation 7

$$I \begin{bmatrix} x_{T+1} - x^* \\ \vdots \\ x_{T+\theta} - x^* \end{bmatrix} = 0 \tag{7}$$

instead of equation 6.

Since Equation 6 more accurately characterizes the dynamics of the nonlinear system near the steady state the approach described in this paper converges more quickly. It will be convenient to normalize the $\mathcal{Q}$ matrix so that there is the negative of the identity matrix in the rightmost block. (Anderson & Moore, 1985) shows that such a normalization exists for models which have uniquely convergent saddle points paths from arbitrary initial conditions.

$$Q^N = \begin{bmatrix} -B_1 & I & & & \\ -B_2 & & I & & \\ \vdots & & & \ddots & \\ -B_{\theta-1} & & & & I \\ -B_\theta & & & & \end{bmatrix} \tag{8}$$

Thus, the traditional approach of setting the end of the trajectory to the steady state would be equivalent to zeroing out the left half of the normalized $\mathcal{Q}$ matrix. Using AIM to Restrict the end of the trajectory to the asymptotic stable linear subspace provides a better approximation of the asymptotic behavior of the non linear function. This improvement in the approximation is reflected in the length of the trajectory needed to achieve a given level of accuracy for the values at the beginning of the trajectory. In order to achieve

a specific number of significant digits in the computation of the points near the beginning of the trajectory, setting the end of the trajectory equal to a specific constant would force us to compute a longer solution path than adopting our approach of restricting the solution to the asymptotic linear space.

2 Two Non-Linear Examples

2.1 A Money Demand Model

Consider the three equation non-linear system

$$\ln \frac{m_t}{p_t} = \alpha + \beta \ln(\rho + (\frac{p_{t+1} - p_t}{p_t})) \tag{9}$$

$$m_t - m_{t-1} = \gamma(m_{t-1} - \mu) + \delta s_t \tag{10}$$

$$s_t = \lambda s_{t-1}(1 - s_{t-1}) \tag{11}$$

Where $L = 3, \tau = 1, \theta = 1$, and $0 \leq \lambda,\ \alpha < 0\ ,\ \beta < 0\ ,\ \rho > 0,\ \gamma < 0$, and $\mu > 0$ exogenously given. This example augments a simple forward looking money demand function(Equation 9) and a money supply rule(Equation 10) with an easy to manipulate and much studied nonlinear function, the quadratic map(Equation 11). Including the quadratic map provides a convenient way to study the impact of model parameters on asymptotic behavior. The parameter λ in the quadratic map provides a simple nonlinear function that can generate fixed points, limit cycles, and chaotic invariant sets, but this paper will study values of λ associated with fixed points.

The points $m^* = \mu - \frac{-\delta s^*}{\gamma}\ p^* = m^* \exp^{-(\alpha + \beta \ln(\rho))}$, where $s^* = 0$ or $s^* = \frac{\lambda - 1}{\lambda}$, are fixed points for the system. We can linearize the system and investigate the dynamics of the system near either steady state.

We want to investigate the model with initial conditions

$$m_0 = \bar{m}_0$$

$$p_0 = \bar{p}_0$$

$$s_0 = \bar{s}_0$$

and terminal conditions

$$\lim_{t\to\infty} \begin{bmatrix} m_t \\ p_t \\ s_t \end{bmatrix} = \begin{bmatrix} m^* \\ p^* \\ s^* \end{bmatrix}$$

Applying the methods of (Anderson & Moore, 1985) near the fixed point, the state space transition matrix is

$$A = \begin{bmatrix} (1+\gamma) & 0 & -\delta\lambda(2s^*-1) \\ \frac{\rho/\beta}{m^*/p^*} & \frac{\beta-\rho}{\beta} & 0 \\ 0 & 0 & -\lambda(2s^*-1) \end{bmatrix}$$

Which has three non zero eigenvalues, $(1+\gamma)$, $\lambda(1-2s^*)$, and $\frac{\beta-\rho}{\beta}$.

The first two eigenvalues are smaller than one in magnitude provided:

$$-2 < \gamma < 0$$

and

$$s^* = \begin{cases} 0 \text{ and } |\lambda| < 1 \\ \frac{\lambda-1}{\lambda} \text{ and } 1 < \lambda < 3 \end{cases}$$

The last eigenvalue has magnitude bigger than one since $\frac{\rho}{\beta} < 0$.

The Q matrix of constraints imposing the saddle point property consists of two auxiliary initial conditions and one unstable left eigenvector if $0 < \lambda < 1$ or $1 < \lambda < 3$

$$Q = \begin{bmatrix} -(1+\gamma) & 0 & 0 & 1 & 0 & -\delta \\ 0 & 0 & \lambda(2s^*-1) & 0 & 0 & 1 \\ 0 & 0 & 0 & -\frac{(-\beta+\beta\lambda+\rho-2\beta\lambda s^*)}{(\beta\delta\lambda(1-s^*))} & -\frac{m^*(\beta\gamma+\rho)(-\beta+\beta\lambda+\rho-2\beta\lambda s^*)}{\rho p^*(\beta\delta\lambda(1-s^*))} & 1 \end{bmatrix}$$

$$Q^N = \begin{bmatrix} 1+\gamma & 0 & \delta\lambda - 2\delta\lambda s^* & -1 & 0 & 0 \\ \frac{(1+\gamma)\rho p^*}{(\beta\gamma+\rho)m^*} & 0 & \frac{\delta\lambda\rho(-\beta+\rho)p^*(-1+2s^*)}{(\beta\gamma+\rho)m^*(\beta-\beta\lambda-\rho+2\beta\lambda s^*)} & 0 & -1 & 0 \\ 0 & 0 & \lambda - 2\lambda s^* & 0 & 0 & -1 \end{bmatrix} \tag{12}$$

$$= \begin{bmatrix} B_1 & -I \end{bmatrix} \tag{13}$$

2.2 Boucekkine's Non Linear Example

Boucekkine's(Boucekkine, 1995) presents the following example nonlinear model. For $t > 0$

$$z_t - 5y_{1,t}^{0.15}x_{1,t}^{0.75} = 0 \tag{14}$$

$$0.15\frac{y_{1,t+1}}{y_{1,t}} + 5x_{1,t}^{a} - 0.25 = 0 \tag{15}$$

$$y_{2,t+1} - 3\frac{y_{2,t}^{1.65}}{x_{1,t-1}}w_{t-3} = 0 \tag{16}$$

$$x_{2,t} - 0.75\frac{y_{1,t-1}}{y_{2,t}} + 1.25 = 0 \tag{17}$$

$$y_{1,t+1}^{b} - c\frac{x_{2,t-1}}{y_{2,t+1}}y_{1,t} = 0 \tag{18}$$

$$w_t = 1 \tag{19}$$

Solving for fixed point solutions x_1^*, x_2^*, y_2^*, z^* in terms of y_1^* produces

$$w_1^* = 1.$$

$$x_1^* = 50.^{\frac{-1.}{a}}$$

$$x_2^* = -1.25 + 4.06531\,50.^{\frac{1.53846}{a}}\,y1$$

$$y_2^* = \frac{0.184488}{50.^{\frac{1.53846}{a}}}$$

$$z^* = \frac{5.\,y1^{\frac{3}{20}}}{50.^{\frac{0.75}{a}}}$$

provided y_1^* satifies

$$y1^{b} - \frac{5.42042\,c\,y1\left(-5. + 16.2613\,50.^{\frac{1.53846}{a}}\,y1\right)^{d}}{4.^{1.\,d}\,50.^{\frac{-1.}{a}\frac{20}{13}}} = 0. \tag{20}$$

Fixing a, b, and c produces a version of the mode whose asymptotic behaviour depends only on d. In the text that follows,

$$\{a \to -3, b \to \frac{3}{2}, c \to \frac{5}{2}\}.$$

Figure 1 graphs solutions for 20 as a function of d. Note that for values of d between 0.0700073 and 0.38472 y_1 is complex valued. This paper will analyze model solutions over the range of d for which the solutions for y_1 are real valued.

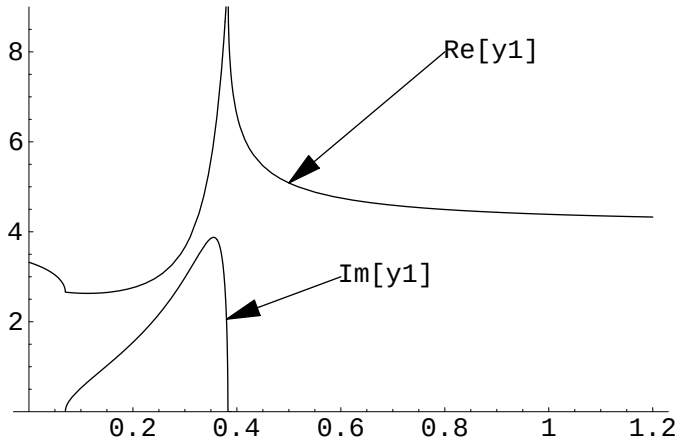

Figure 1: y1 Solutions versus d with $\{a \to -3, b \to \frac{3}{2}, c \to \frac{5}{2}\}$

In constructing the transition matrix, the AIM algorithm discovers 4 auxiliary initial conditions. Figure 2 graphs the magnitude of the second and third largest eigenvalues as a function of d. The model will have locally unique convergent solutions when there are exactly two eigenvalues with magnitudes bigger than one. When the second largest eigenvalue has a magnitude less than one, there are multiple solutions converging to the steady state. When the third largest eigenvalue has a magnitude greater than one, there are no solutions converging to the steady state.

Table 1 displays the eigenvalues for the asymptotic linearization when $d = 1.0$. Since there are 4 roots with magnitudes larger

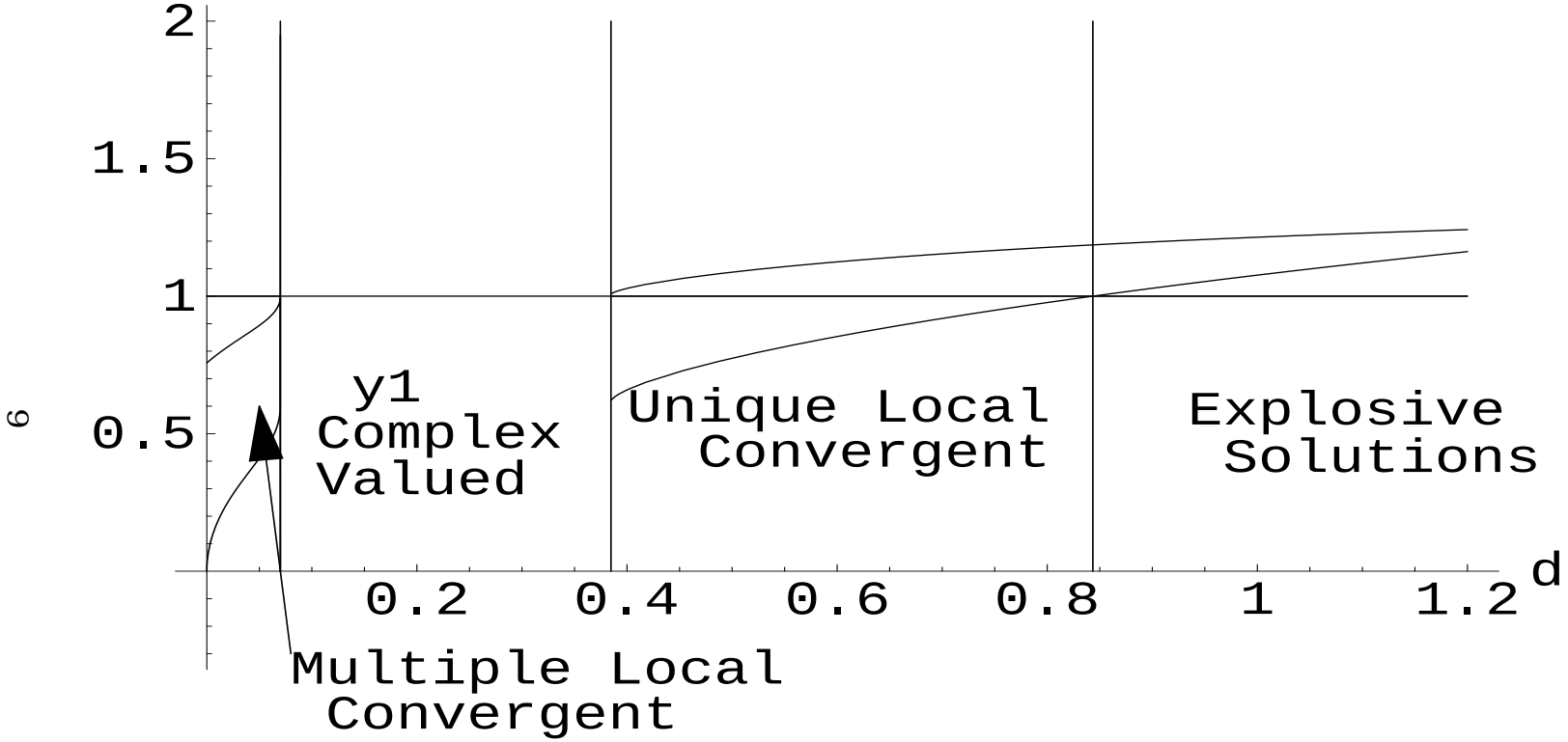

Figure 2: Magnitude of Second and Third Largest Eigenvalues versus d

than one and 4 auxiliary initial conditions, there are no solutions converging to the fixed point from arbitrary initial starting points.

Fixed Point	$\{1., 3.68403, 1.14926, 4.38784, 1.37162, 16.5978\}$
Eigenvalues	$\{2.12643, -0.345383 - 1.01957\,i, 1.21433, -0.345383 + 1.01957\,i\}$
Magnitudes	$\{2.12643, 1.07649, 1.21433, 1.07649\}$

Table 1: Solution characteristics for d=1.0

Table 2 displays the eigenvalues for the asymptotic linearization when $d = 0.05$. Since there are 4 auxiliary initial conditions and only one eigenvalue with magnitude greater than one, there are multiple solutions converging to the fixed point.

Fixed Point	$\{1., 3.68403, 0.412629, 3.04066, 1.37162, 15.7093\}$
Eigenvalues	$\{1.91557, -0.0795795 - 0.402948\,i, 0.893593, -0.0795795 + 0.402948\,i\}$
Magnitudes	$\{1.91557, 0.410731, 0.893593, 0.410731\}$

Table 2: Solution characteristics for d=0.05

Table 3 displays the eigenvalues for the asymptotic linearization when $d = 0.5$. Since there are 4 auxiliary initial conditions and two eigenvalues with magnitude greater than one, so long as the auxiliary initial conditions and the eigenvectors associated with the two roots with magnitudes greater than one are linearly independent, there are unique solutions converging to the steady state from arbitrary initial conditions. Table 4 on page 11. presents the $\mathcal{Q}$ and normalized $\mathcal{Q}$ matrices.

Fixed Point	$\{1., 3.68403, 1.53089, 5.08577, 1.37162, 16.9694\}$
Eigenvalues	$\{1.99626, -0.216796 - 0.743478\,i, 1.08733, -0.216796 + 0.743478\,i\}$
Magnitudes	$\{1.99626, 0.774441, 1.08733, 0.774441\}$

Table 3: Solution characteristics for d=0.5

Appendix B provides additional detail describing the transition matrix and the auxiliary initial conditions.

$$Q = \begin{bmatrix} 0 & 0 & 0 & 0 & 0 \\ 0 & 0 & 0 & 0 & 0 \\ 0 & 0 & 0 & 0 & 0 \\ 0 & 0 & 0 & 0 & 0 \\ 0 & -0.345841 & 0 & 0 & 0 \\ 0 & -0.490676 & 0 & 0 & 0 \end{bmatrix} \cdots \begin{bmatrix} 0 & 0 & 0 & 0 & 0 \\ 0 & 0 & 0 & 0 & 0 \\ 0 & 0 & 0 & 0 & 0 \\ 0 & 0 & 0 & 0 & 0 \\ 0 & -0.345841 & 0 & 0 & 0 \\ 0 & -0.490676 & 0 & 0 & 0 \end{bmatrix}$$

$$Q^N = \begin{bmatrix} 0 & 0 & 0 & 0 & 0 & 0 & 0 & 0 & 0 & 0 & 0 & 0 & 0 & 0 & 0 & 0 & 0 & -1 & 0 & 0 & 0 & 0 & 0 \\ 0.0569869 & 0 & 0 & 0 & 0 & 0 & 0.883257 & 0 & 0 & 0 & 0 & 0 & 0.66277 & -0.0154686 & 0.422866 & 0.0184885 & 0 & 0 & 0 & -1 & 0 & 0 & 0 & 0 \\ 1.59759 & 0 & 0 & 0 & 0 & 0 & 0.743066 & 0 & 0 & 0 & 0 & 0 & 0.319599 & -0.433653 & -0.0930743 & 0.518313 & 0 & 0 & 0 & 0 & -1 & 0 & 0 & 0 \\ -1.0019 & 0 & 0 & 0 & 0 & 0 & -2.83148 & 0 & 0 & 0 & 0 & 0 & -3.56087 & 0.271957 & -0.742194 & -0.32505 & 0 & 0 & 0 & 0 & 0 & -1 & 0 & 0 \\ -0.78798 & 0 & 0 & 0 & 0 & 0 & -0.366502 & 0 & 0 & 0 & 0 & 0 & -0.157636 & 0.213891 & 0.0459071 & 0.0140497 & 0 & 0 & 0 & 0 & 0 & 0 & -1 & 0 \\ -0.304576 & 0 & 0 & 0 & 0 & 0 & 1.6342 & 0 & 0 & 0 & 0 & 0 & 0.507439 & 0.0826745 & 1.08939 & -0.0988148 & 0 & 0 & 0 & 0 & 0 & 0 & 0 & -1 \end{bmatrix}$$

Table 4: Asymptotic Linear Constraints for Boucekkine Example: $(\{a \to -3, b \to \frac{3}{2}, c \to \frac{5}{2}, d \to 0.5\})$

3 Components of the Algorithm for Computing the Convergent Path

One can apply Newton's Algorithm to compute the solution to the non linear system Equations 1-3. With

$$y_t = \begin{bmatrix} x_{t-\tau} \\ x_{t-\tau+1} \\ \vdots \\ x_{t+\theta-1} \\ x_{t+\theta} \end{bmatrix} \tag{21}$$

$$z(T) = \begin{bmatrix} x_{-\tau} \\ x_{-\tau+1} \\ \vdots \\ x_{T+\theta-1} \\ x_{T+\theta} \end{bmatrix} \tag{22}$$

Equations 1-3 become

$$\aleph(z(T), \mho) = \begin{bmatrix} \begin{bmatrix} x_{-\tau} - \bar{x}_{-\tau} \\ \vdots \\ x_{-1} - \bar{x}_{-1} \end{bmatrix} \\ h(y_1) \\ h(y_2) \\ \vdots \\ h(y_{T-1}) \\ h(y_T) \\ \mho \begin{bmatrix} x_{T+1-\tau} - x^* \\ \vdots \\ x_{T+\theta} - x^* \end{bmatrix} \end{bmatrix} \text{ where } \mho = \begin{cases} Q & \text{for AIM} \\ \begin{bmatrix} 0 & I \end{bmatrix} & \text{for FP} \end{cases} \tag{23}$$

Figures 3 and 4 present pseudo code describing the algorithms for analyzing the steady state and computing the convergent path.

3.1 Improved Model Diagnostics

It is possible to choose the parameters of the model and initial conditions so that the number of time periods to convergence is

```
begin
  if ¬succeedsQ(xStar := computeFixedPoint(h, xGuessFP))
    then fail comment: unable to compute fixed point
     else H := linearize(h, xStar)
          if ¬hasSaddlePointPropertyQ(Q := andersonMoore(H))
            then fail comment: no saddle point property at this fixed point
             else
                  if ¬hasConvergedQ(xPath :=
                    convergentPath(xHistory, h, Q, T_MIN, T_MAX))
                    then fail comment: path has yet to converge
                     else success(xPath)
                  fi
          fi
  fi
end
```

Figure 3: Nonlinear Extension of Anderson-Moore Algorithm: Initial Setup

```
begin
  T := T_MIN
  xPathOld := solveNonLinearSystem(xHistory, h, Q, T_MIN, xGuessPath)
  T := T + ΔT
  xPathNew := solveNonLinearSystem(xHistory, h, Q, T)
  while (xPathOld ≠ xPathNew) ∧ (T ≤ T_MAX) do
        xPathOld := xPathNew
        T := T + ΔT
        xPathNew := solveNonLinearSystem(xHistory, h, Q, T) od
end
```

Figure 4: Nonlinear Extension of Anderson-Moore Algorithm: convergentPath

arbitrarily large. Thus, for some parameter settings, procedures which depends on failure to converge will have trouble determining the appropriateness of the asymptotic stability conditions. The asymptotic linearization approach provides this information near the beginning of computation before undertaking many costly computations leading to uncertain results.

3.1.1 Computational Results

The approach of this paper focuses computational resources on computing saddle point paths for models which have saddle point paths. The analysis of the previous section indicates that the money demand model will have convergent perfect foresight paths to the $s = 0$ fixed point for $0 < \lambda < 1$ and to the $s = \frac{\lambda-1}{\lambda}$ for $1 < \lambda < 3$. There is no need to attempt solutions for models with values of λ outside this range.

The analysis of the previous section indicates that the Boucekkine model will have convergent perfect foresight paths for $0.38472 < d < 0.843407$. There is no need to attempt solutions for models with values of d outside this range.

3.2 Improved Initial Path Guess

The Newton iteration requires an initial guess, $z^0(T)$. Define

$$z^*(T^0, \mho) \ni \aleph(z^*(T^0, \mho), \mho) = 0 \tag{24}$$

The $z^*(T^0, \mho)$ represent solutions to Equation 21 using T^0 non linear time periods before applying asymptotic constraint $\mho$. Using iterative techniques to get a solution for $z^*(T, \mho), T > T^0$ will require an initial guess $z^0(T)$

3.2.1 Steady State Bootstrap

The traditional approach augments the shorter solution trajectory $z^0(T^0)$ with the fixed point values.

$$z^0(T) = \begin{bmatrix} z^*(T^0, \begin{bmatrix} 0 & I \end{bmatrix}) \\ x^*_{T^0+1} \\ x^*_{T^0+2} \\ \vdots \\ x^*_{T+\theta-1} \\ x^*_{T+\theta} \end{bmatrix} \tag{25}$$

3.2.2 Aim Bootstrap

Alternatively, one could augment the shorter solution trajectory $z^0(T^0)$ with values consistent with the asymptotic behavior of the non linear system near the fixed point.

$$z^0(T) = \begin{bmatrix} z^*(T^0, Q) \\ \hat{x}_{T^0+1} \\ \hat{x}_{T^0+2} \\ \vdots \\ \hat{x}_{T+\theta-1} \\ \hat{x}_{T+\theta} \end{bmatrix} \tag{26}$$

with

$$\hat{x}_t = x^* + B_1 \begin{bmatrix} (\hat{x}_{t-\tau} - x^*) \\ \vdots \\ (\hat{x}_{t-1} - x^*) \end{bmatrix} \forall t > T_0 \tag{27}$$

Where B_1 comes from the first few rows of Q^N of equation 12 on page 6.

Appendix A presents equations describing the AIM bootstrap applied to the Money Demand Model.

3.2.3 Computational Results

Using B_1 reduces the number of Newton steps required to compute a path of given horizon length whether or not using Q for the

asymptotic constraint. Figure 5 and 6 show the number of newton steps needed to move from the initial guess to the solution for each horizon length. The line labeled "FP Initialization" shows the number of steps required when setting the entire initial path guess to the fixed point values. The line labeled "Q Initialization" shows the number of steps required when setting the initial path guess to the result of applying the B_1 matrix to the initial conditions given in equation 2. The line labeled "FP Extension" shows the number of steps required when applying the Steady State Bootstrap to the solution from a horizon on period shorter. The line labeled "Q Extension" shows the number of steps required when applying the AIM Bootstrap to the solution from a horizon one period shorter. The "Q Extension" and "Q Initialization" lines show the number of Newton steps required to solve equation 24 with $\mho = Q$. The "FP Extension" and "FP Initialization" lines show the number of Newton steps required to solve equation 24 with $\mho = \begin{bmatrix} 0 & I \end{bmatrix}$. These results are typical for applying the two initial path guess strategies to the two models.

The AIM Bootstrap minimizes the number of Newton steps for finding the $z^*(T, \mho)$ for both models. Figure 5 presents computational results for the Money Demand Model. For example, Figure 5 indicates that at a horizon of 5 periods, initializing the path to the steady state lead to 13 newton steps. Initializing the path to the solution obtained by applying the asymptotic linearization to the initial conditions alone lead to 7 Newton steps. Extending the 4 period solution by adding one period of fixed point values leads to 5 Newton steps. Using AIM to augment the 4 period solution leads to 3 Newton Steps.

Figure 6 presents computational results for the Boucekkine Model. Figure 6 indicates that at a horizon of 7 periods, initializing the path to the steady state lead to 5 newton steps. Initializing the path to the solution obtained by applying the asymptotic linearization to the initial conditions alone lead to 4 Newton steps. Extending the 6 period solution by adding one period of fixed point values leads to 3 Newton steps. Using AIM to augment the 6 period solution leads to 3 Newton Steps. Extending the path using the Fixed Point Bootstrap or the AIM Bootstrap lead to the same number of Newton

steps. The next section will show that the AIM Bootstrap dominates since the "FP" algorithms require more iterations to converge to the same accuracy than the "Q" algorithms.

3.3 Shorter Computation Horizon for Given Computation Error

When solving models with the saddle point property near the steady state, the two approaches compute equivalent paths. However, using Q improves the tradeoff between computation horizon and solution accuracy. For a given level of precision, the asymptotic linearization approach obtains the solution with a shorter computation horizon. At any given computation horizon, the asymptotic linearization approach computes a more accurate solution.

This paper defines numerical convergence for the algorithms using a measure of relative error. The algorithms terminate when

$$\|D^T(x - \hat{x})\| \leq m\|D^T\hat{x}\|$$

where

$$D^T = \begin{cases} \{1., 1., 1.\} & \text{Money Demand Model} \\ \{1., 0.27144, 0.65321, 0.19663, 0.72906, 0.05893\} & \text{Boucekkine Model} \end{cases}$$

$$\|\epsilon\| = \sqrt{(\epsilon^T\epsilon)}$$

$$x - \hat{x} = S_{1k}z^k(T) - S_{2k}z^{k-1}(T)$$

$$\text{with } S_{1k} = \begin{bmatrix} I_{nL} & 0 \end{bmatrix} \text{ and } S_{2k} = \begin{bmatrix} I_{nL} & 0 \end{bmatrix}$$

chosen to select comparable parts of the state vector.

If $m = 10^{-k}$ then larger components of Dx have k significant digits(Numerical Algorithms Group, 1995). The numerical calculation for this paper set $k \approx 8$.

3.3.1 Computational Results

Table 5 presents some computational results for the Money Demand Model. The last column demonstrates the equivalence between the convergent solution paths obtained by using the asymptotic linearization and those obtained using the traditional fixed

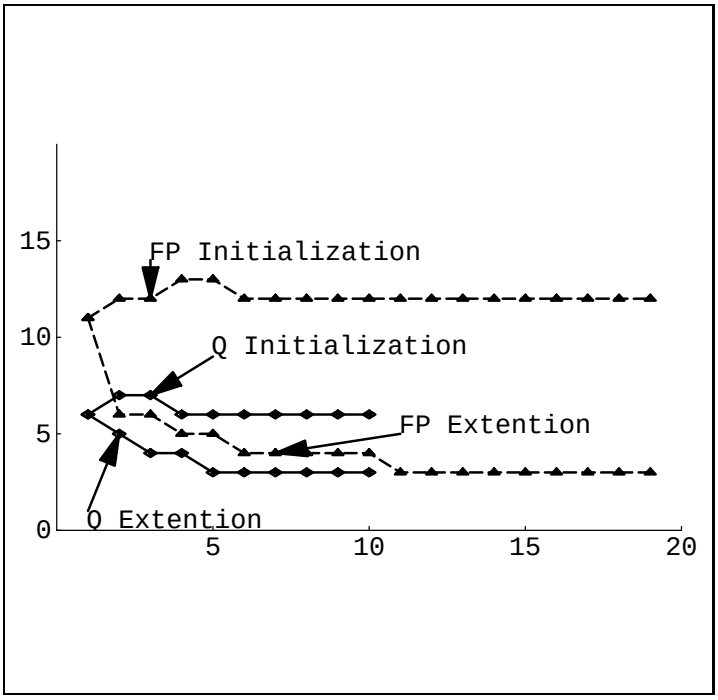

Figure 5: Newton Steps as Function of Horizon Length for Various Initial Guesses for Money Demand Model

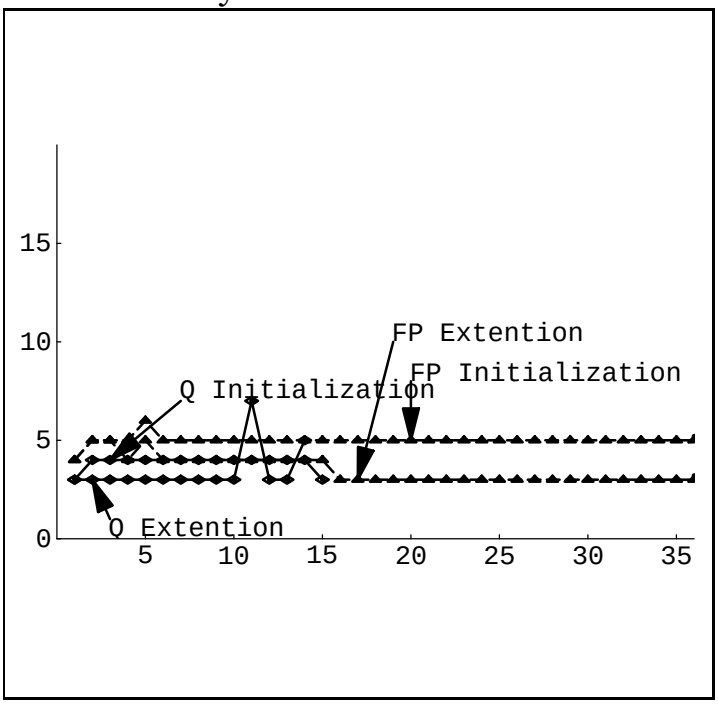

Figure 6: Newton Steps as Function of Horizon Length for Various Initial Guesses for Boucekkine Model

point constraint. The computations using $\mathcal{Q}$ and using FP each used a convergence tolerance of $10^{-}8$. The $\|\cdot\|_2$ difference between the initial portions of the trajectories are also within the supplied convergence tolerance of 10^{-8}.

λ	Fixed Point	Largest EVal	Convergence		$\|x_Q - x_{FP}\|$
			$\mathcal{Q}$	FP	
1.5	$0.467, 0.693, 0.333$	0.5	11	22	$2.17835\,10^{-9}$
1.9	$0.242, 0.359, 0.474$	0.1	10	19	$4.45944\,10^{-9}$
2.3	$0.0957, 0.142, 0.565$	-0.3	9	18	$2.43792\,10^{-9}$

Table 5: Asymptotic Linearization and Fixed Point Solution Characteristics

The following figures employ two measures of error to characterize the rate of convergence of the two algorithms: approximation error and change in path error. The approximation error is $\|D(S_{1k}(T)x_{now} - S_{2k}(T^*)x_{converged})\|_2$. The change in path error is $\|D(S_{1k}(T+1)x_{next} - S_{2k}(T)x_{now})\|_2$.

The top half of Figure 7 reports the variation in approximation error as a function of the computation horizon when $\lambda = 1.5$. For any given horizon, the approximation error is always about 6 times larger when using the fixed point instead of the asymptotic linearization. The bottom half of Figure 7 emphasizes this point by reporting the variation in approximation rescaled so that the initial approximation errors are the same.

Without prior knowledge of the convergent solution, algorithms rely on the change in the solution path to determine convergence. Figure 8 reports the variation in the change in path error as a function of the computation horizon when $\lambda = 1.5$. The asymptotic linearization algorithm would signal convergence before the fixed point algorithm. The accuracy of the solution does not suffer since the aggregate errors are so much less for any given computation horizon.

Figure 9 reports the variation in approximation error as a function of the computation horizon when $\lambda = 1.9$. Again, for any given horizon, the approximation error is always significantly less when using the asymptotic linearization. Figure 10 reports the variation

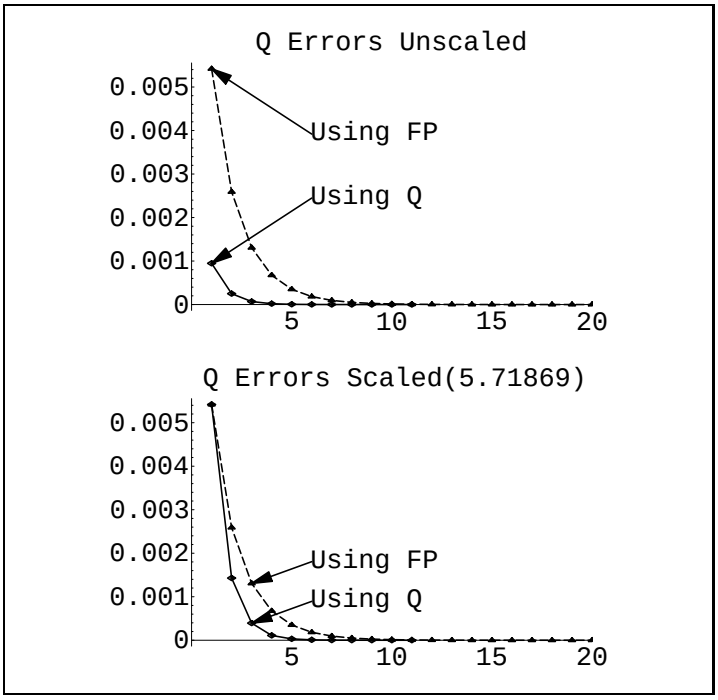

Figure 7: Approximation Error as Function of T for $\lambda = 1.5$

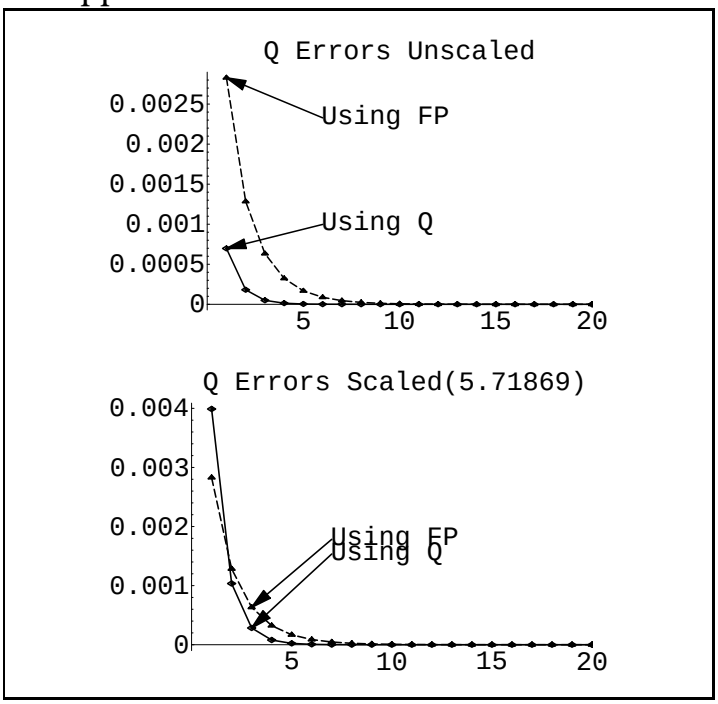

Figure 8: Change in Path Error as Function of T for $\lambda = 1.5$

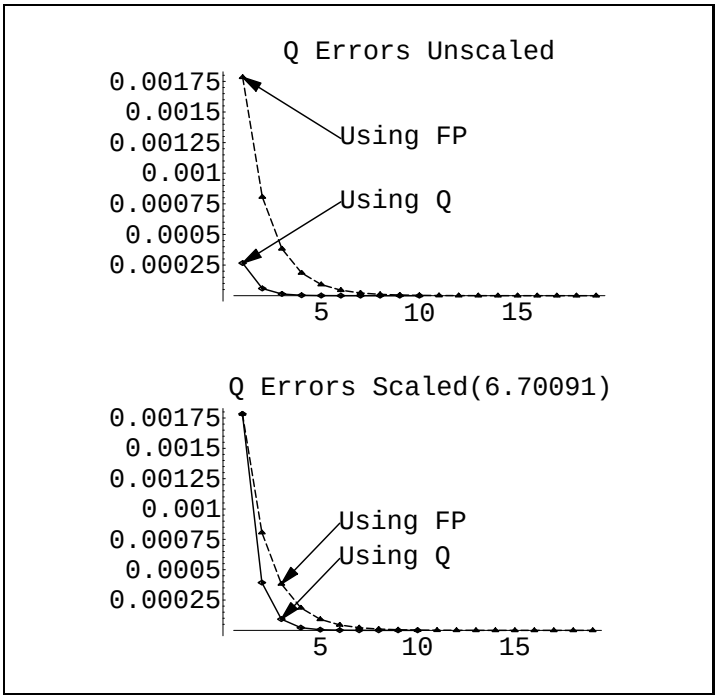

Figure 9: Approximation Error as Function of T for $\lambda = 1.9$

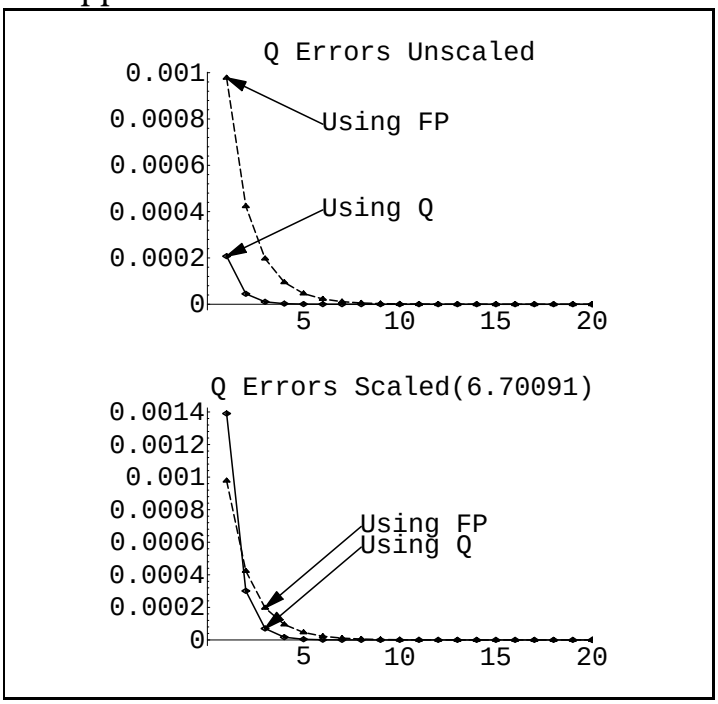

Figure 10: Change in Path Error as Function of T for $\lambda = 1.9$

in the change in approximation error as a function of the computation horizon when $\lambda = 1.9$. The asymptotic linearization algorithm would signal convergence before the fixed point algorithm.

Figure 11 reports the variation in approximation error as a function of the computation horizon when $\lambda = 2.3$. For any given horizon, the approximation error is always significantly less when using the asymptotic linearization. Figure 12 reports the variation in the change in approximation error as a function of the computation horizon when $\lambda = 2.3$. The asymptotic linearization algorithm would signal convergence before the fixed point algorithm.

Figure 13 presents a density plot comparing the number of horizons required for convergence for the two algorithms as a function of the initial conditions. Since m_0 and s_0 depend only on initial conditions they will not vary as the horizon length, T_0, changes, but p_0 will depend on the future values and the terminal conditions and will vary with the horizon length. The asymptotic linearization converges faster than the fixed point for all initial conditions.

Figures 14 -16 present some computational results for the Boucekkine Model. Figure 14 reports the approximation error while Figure 15 reports the variation in the change in approximation error as a function of the computation horizon when $d = 0.5$ For any given horizon, the approximation error is always significantly less when using the asymptotic linearization. The asymptotic linearization algorithm would signal convergence before the fixed point algorithm. The accuracy of the solution does not suffer since the aggregate errors are so much less for any given computation horizon.

Figure 16 presents a graph comparing the number of horizons required for convergence for the two algorithms as a function of the initial conditions for w. The asymptotic linearization converges faster than the fixed point for all initial conditions.

4 Conclusions

Linearizing non linear models about their steady state makes it possible to use the Anderson-Moore Algorithm(AIM) to investigate their saddle point properties and to efficiently compute their solutions. Using AIM to check the long run dynamics of non linear

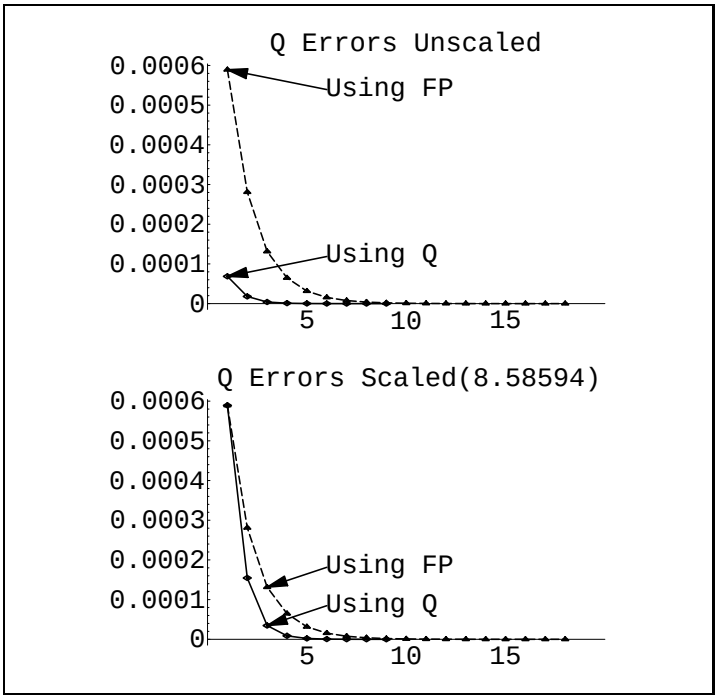

Figure 11: Approximation Error as Function of T for $\lambda = 2.3$

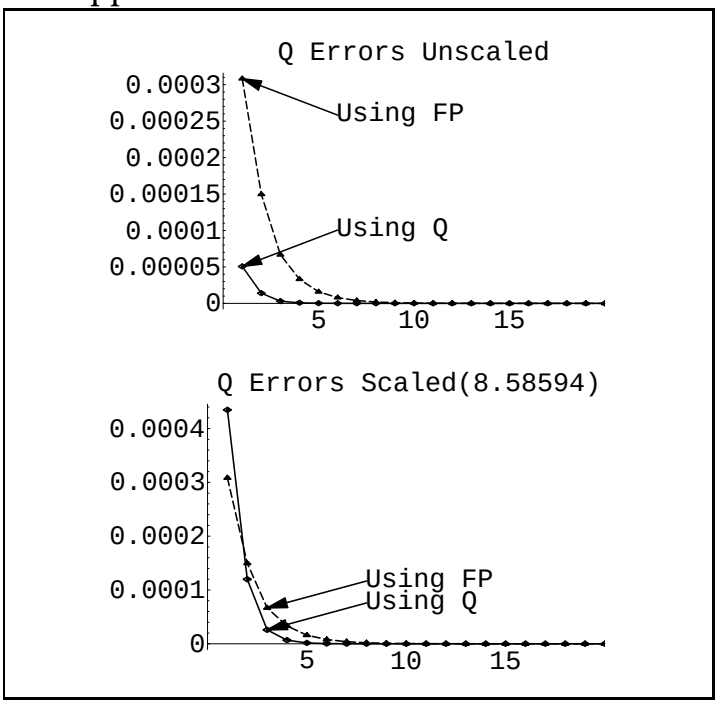

Figure 12: Change in Path Error as Function of T for $\lambda = 2.3$

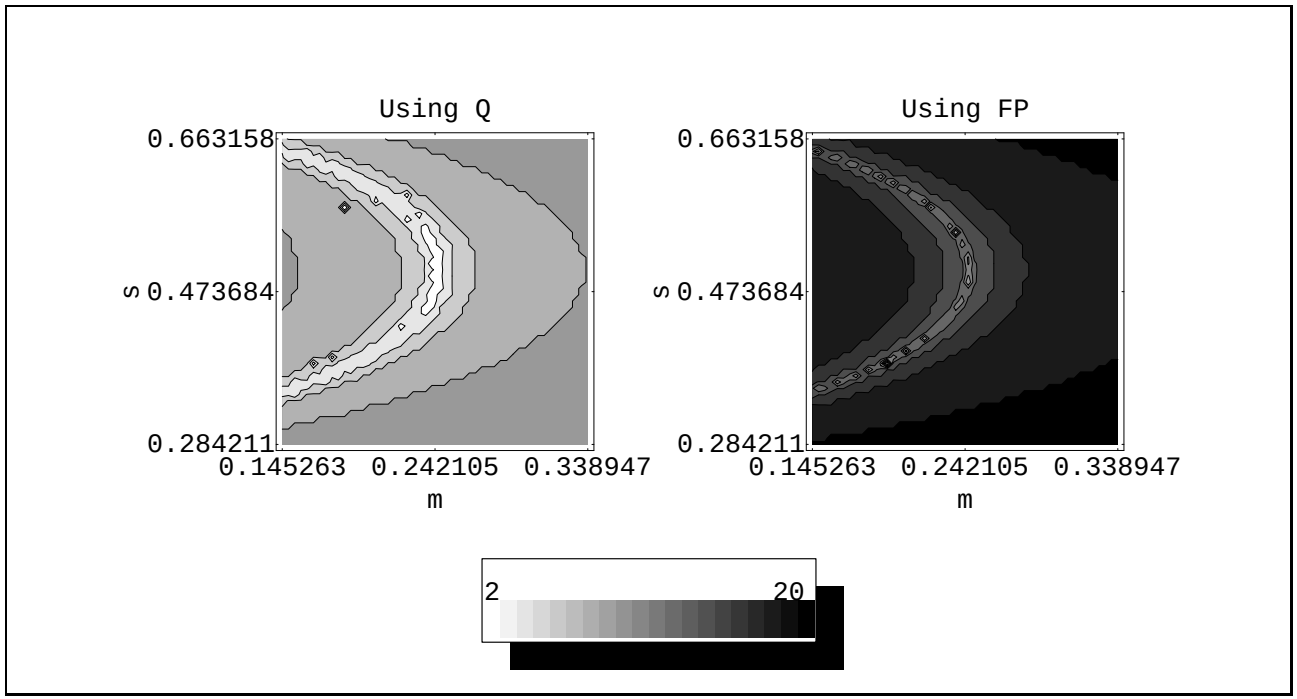

Figure 13: Horizon Length as a Function of Initial Conditions

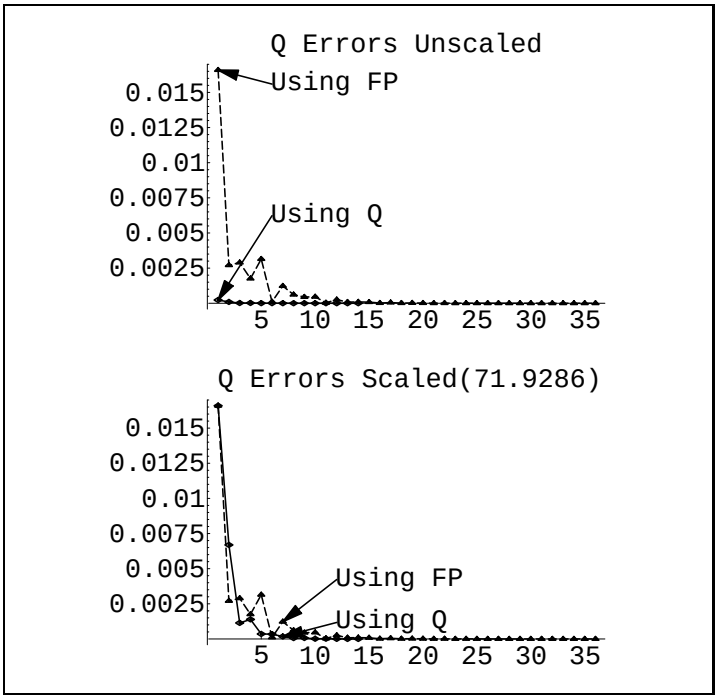

Figure 14: Variation in Approximation Error as Function of T for $a = -3, b = \frac{3}{2}, c = \frac{5}{2}, d = \frac{1}{2}$

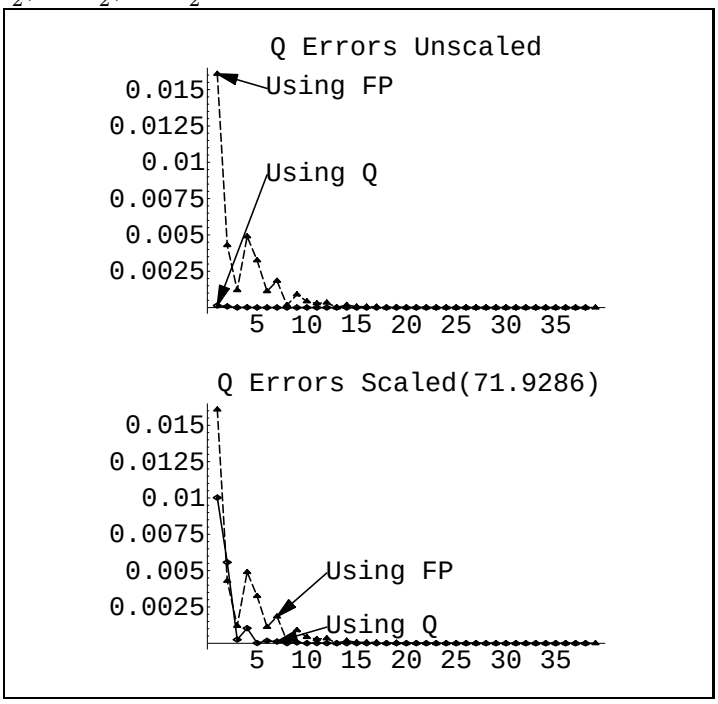

Figure 15: Change in Path Error as Function of T for $a = -3, b = \frac{3}{2}, c = \frac{5}{2}, d = \frac{1}{2}$

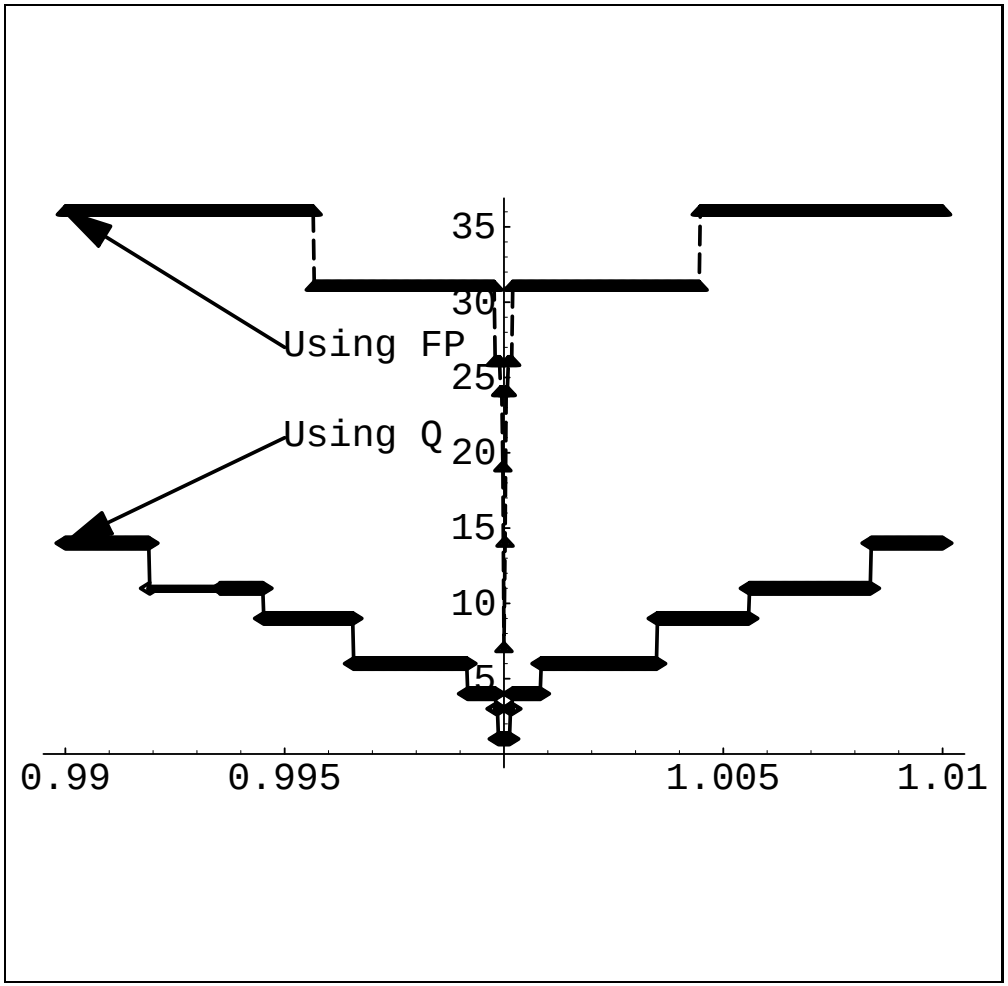

Figure 16: Horizon Length Versus Distance to Steady State

models avoids many of the burdensome computations associated with alternative methods for verifying the saddle point property. In addition, for models that have the saddle point property, AIM provides a set of terminal conditions for solving the non linear model that work better than the traditional approach of setting the end of the trajectory to the steady state values. Furthermore, the asymptotic linear constraints can also generate initial conditions for the solution path that are better than initializing the solution path to the steady state values. Using the improved asymptotic constraints typically halves the computational burden associated with solving the nonlinear problem.

References

Anderson, Gary, & Moore, George. 1985. A Linear Algebraic Procedure For Solving Linear Perfect Foresight Models. *Economics Letters*, **17**.

Boucekkine, Raouf. 1995. An Alternative Methodology for Solving Nonlinear Forward-Looking Models. *Journal of Economic Dynamics and Control*, **19**, 711–734.

Fair, Ray, & Taylor, John. 1983. Solution and Maximum Likelihood Estimation of Dynamic Rational Expectations Models. *Econometrica*, **51**.

Fuhrer, Jeffrey C., & Bleakley, C. Hoyt. 1996. *Computationally Efficient Solution and Maximum Likelihood Estimation of Nonlinear Rational Expectations Models*. Tech. rept. Federal Reserve Bank of Boston.

Guckenheimer, John, & Holmes, Philip. 1983. *Nonlinear Oscillations, Dynamical Systems, and Bifurcations of Vector Fields*. Springer-Verlag.

Numerical Algorithms Group. 1995. *C05PCF- NAG Fortran Library Routine Document*. 14 edn.

A Aim Bootstrap Example

For $T^0 = 0$ we can use Equation 12 to compute $\hat{x}_0, \hat{x}_1 \ldots$ for arbitrary initial conditions:

$$\hat{x}_0 = B_1 \begin{bmatrix} (\bar{m}_{-1} - x^*) \\ (\bar{p}_{-1} - p^*) \\ (\bar{s}_{-1} - s^*) \end{bmatrix} = \begin{bmatrix} (1+\gamma)(\bar{m}_{-1} - m^*) + \delta(\bar{s}_{-1} - s^*)\lambda(1-2s^*) \\ \frac{(1+\gamma)(\bar{m}_{-1} - m^*)p^*\rho}{m^*(\beta\gamma+\rho)} + \frac{\delta(\bar{s}_{-1} - s^*)\lambda(1-2s^*)p^*\rho(\rho-\beta)}{m^*(\beta\gamma+\rho)(\beta-\beta\lambda-\rho+2\beta\lambda s^*)} \\ (\bar{s}_{-1} - s^*)\lambda(1-2s^*) \end{bmatrix}$$

$$\hat{x}_1 = B \begin{bmatrix} \hat{m}_0 \\ \hat{p}_0 \\ \hat{s}_0 \end{bmatrix} = \begin{bmatrix} (1+\gamma)(\hat{m}_0 - m^*) + \delta(\hat{s}_0 - s^*)\lambda(1-2s^*) \\ \frac{(1+\gamma)(\hat{m}_0 - m^*)p^*\rho}{m^*(\beta\gamma+\rho)} + \frac{\delta(\hat{s}_0 - s^*)\lambda(1-2s^*)p^*\rho(\rho-\beta)}{m^*(\beta\gamma+\rho)(\beta-\beta\lambda-\rho+2\beta\lambda s^*)} \\ (\hat{s}_0 - s^*)\lambda(1-2s^*) \end{bmatrix}$$

$$\vdots$$

Since the eigenvalues of B_{-1} are $(1+\gamma)$ and $\lambda(1-2s^*)$ the bootstrap path ultimately converges to the steady state. The bootstrap path approximation to the non linear solution improves as the solution approaches the steady state.

For $T^0 = 1$ after substituting the initial conditions and the AIM bootstrap path, we must find m_0, p_0, s_0 satisfying the system

$$-\alpha + \log(\frac{m_0}{p_0}) - \beta \log(\rho + \frac{\frac{(1+\gamma)p^*\rho m_0}{m^*(\beta\gamma+\rho)} - p_0 + \frac{\delta\lambda p^*\rho(\rho-\beta)(2s^*-1)s_0}{m^*(\beta\gamma+\rho)(\beta-\beta\lambda-\rho+2\beta\lambda s^*)}}{p_0}) = 0$$

$$-\bar{m}_{-1} - \gamma\bar{m}_{-1} + \gamma\mu + m_0 - \delta s_0 = 0$$

$$-(\bar{s}_{-1}\lambda) + \bar{s}_{-1}\lambda + s_0 = 0$$

B Transition Matrix Details

$$
\begin{bmatrix}
0 & 0 & 0 & 0 & 0 & 0 & 1. & 0 & 0 & 0 & 0 & 0 & 0 & 0 & 0 \\
0 & 0 & 0 & 0 & 0 & 0 & 0 & 1. & 0 & 0 & 0 & 0 & 0 & 0 & 0 \\
0 & 0 & 0 & 0 & 0 & 0 & 0 & 0 & 1. & 0 & 0 & 0 & 0 & 0 & 0 \\
0 & 0 & 0 & 0 & 0 & 0 & 0 & 0 & 0 & 1. & 0 & 0 & 0 & 0 & 0 \\
0 & 0 & 0 & 0 & 0 & 0 & 0 & 0 & 0 & 0 & 1. & 0 & 0 & 0 & 0 \\
0 & 0 & 0 & 0 & 0 & 0 & 0 & 0 & 0 & 0 & 0 & 1. & 0 & 0 & 0 \\
0 & 0 & 0 & 0 & 0 & 0 & 0 & 0 & 0 & 0 & 0 & 0 & 1. & 0 & 0 \\
0 & 0 & 0 & 0 & 0 & 0 & 0 & 0 & 0 & 0 & 0 & 0 & 0 & 1. & 0 \\
0 & 0 & 0 & 0 & 0 & 0 & 0 & 0 & 0 & 0 & 0 & 0 & 0 & 0 & 1. \\
0 & 0 & 0 & 0 & 0 & 0 & 0 & 0 & 0 & 0 & 0 & 0 & 0 & 0 & 0 \\
0 & 0 & 0 & 0 & 0 & 0 & 0 & 0 & 0 & 0 & 0 & 0 & 0 & 0 & 0 \\
0 & 0 & 0 & 0 & 0 & 0 & 0 & 0 & 0 & 0 & 0 & 0 & 0 & 0 & 0 \\
0 & 0 & 0 & 0 & 0 & 0 & 0 & 0 & 0 & 0 & 0 & 0 & 0 & 0 & 0 \\
0 & 0 & 0 & 0 & 0 & 0 & 0 & 0 & 0 & 0 & 0 & 0 & 0 & 0 & 0 \\
0 & 0 & 0 & 0 & 0 & 0 & 0 & 0 & 0 & 0 & 0 & 0 & 0 & 0 & 0 \\
0 & 0 & 0 & 0 & 0 & 0 & 0 & 0 & 0 & 0 & 0 & 0 & 0 & 0 & 0 \\
0 & 0 & 0 & 0 & 0 & 0 & 0 & 0 & 0 & 0 & 0 & 0 & 0 & 0 & 0 \\
0 & 0 & 0 & 0 & 0 & 0 & 0 & 0 & 0 & 0 & 0 & 0 & 0 & 0 & 0 \\
0 & 0 & 0 & 0 & 0 & 0 & 0 & 0 & 0 & 0 & 0 & 0 & 0 & 0 & 0 \\
-1.61688 & 0 & 0 & 0 & 0 & 0 & -1.22801 & 0 & 0 & 0 & 0 & 0 & 0 & 0.438889 & \frac{-1.689852.^{0.820513-2.d}d(-5.+2.18719\,\mathrm{y1}(d))^{-1.+d}}{\sqrt{\mathrm{y1}(d)}} \\
-0.546798\,\mathrm{y1}(d) & 0 & 0 & 0 & 0 & 0 & 0 & 0 & 0 & 0 & 0 & 0 & 0 & 0.148424\,\mathrm{y1}(d) & 0 \\
-0.666667\,\mathrm{y1}(d) & 0 & 0 & 0 & 0 & 0 & 0 & 0 & 0 & 0 & 0 & 0 & 0 & 0.180961\,\mathrm{y1}(d) & 1.733762.^{1.48718-2.d}d\sqrt{\mathrm{y1}(d)}(-5.+2.18719\,\mathrm{y1}(d))^{-1.+d} \\
1.37162 & 0 & 0 & 0 & 0 & 0 & 0 & 0 & 0 & 0 & 0 & 0 & 0 & -0.372315 & 0 \\
-5.70609\mathrm{y1}(d)^{\frac{3}{20}} & 0 & 0 & 0 & 0 & 0 & -3.32393\mathrm{y1}(d)^{\frac{3}{20}} & 0 & 0 & 0 & 0 & 0 & 0 & 1.54887\mathrm{y1}(d)^{\frac{3}{20}} & \frac{3.876812.^{-1.26282-2.d}d(-5.+2.18719\,\mathrm{y1}(d))^{-1.+d}}{\mathrm{y1}(d)^{\frac{7}{20}}}
\end{matrix}\cdots
$$

$$
\begin{matrix}
0 & 0 & 0 & 0 & 0 & 0 & 0 & 0 & 0 \\
0 & 0 & 0 & 0 & 0 & 0 & 0 & 0 & 0 \\
0 & 0 & 0 & 0 & 0 & 0 & 0 & 0 & 0 \\
0 & 0 & 0 & 0 & 0 & 0 & 0 & 0 & 0 \\
0 & 0 & 0 & 0 & 0 & 0 & 0 & 0 & 0 \\
0 & 0 & 0 & 0 & 0 & 0 & 0 & 0 & 0 \\
0 & 0 & 0 & 0 & 0 & 0 & 0 & 0 & 0 \\
0 & 0 & 0 & 0 & 0 & 0 & 0 & 0 & 0 \\
0 & 0 & 0 & 0 & 0 & 0 & 0 & 0 & 0 \\
1. & 0 & 0 & 0 & 0 & 0 & 0 & 0 & 0 \\
0 & 1. & 0 & 0 & 0 & 0 & 0 & 0 & 0 \\
0 & 0 & 1. & 0 & 0 & 0 & 0 & 0 & 0 \\
0 & 0 & 0 & 1. & 0 & 0 & 0 & 0 & 0 \\
0 & 0 & 0 & 0 & 1. & 0 & 0 & 0 & 0 \\
0 & 0 & 0 & 0 & 0 & 1. & 0 & 0 & 0 \\
0 & 0 & 0 & 0 & 0 & 0 & 1. & 0 & 0 \\
0 & 0 & 0 & 0 & 0 & 0 & 0 & 1. & 0 \\
0 & 0 & 0 & 0 & 0 & 0 & 0 & 0 & 1. \\
0 & 0 & 0 & 0 & 0 & 0 & 0 & 0 & 0 \\
0 & 0 & 0 & 0 & 0.333333 & \frac{5.069552.^{0.820513-2.d}d(-5.+2.18719\,\mathrm{y1}(d))^{-1.+d}}{\sqrt{\mathrm{y1}(d)}} & \frac{-0.409337}{\mathrm{y1}(d)} & -1.94504 & 0 \\
0 & 0 & 0 & 0 & 0 & 0 & 0.546798 & -0.657775\,\mathrm{y1}(d) & 0 \\
0 & 0 & 0 & 0 & 0 & 0 & 0.666667 & -0.801971\,\mathrm{y1}(d) & 0 \\
0 & 0 & 0 & 0 & 0 & 0 & 0 & 1.65 & 0 \\
0 & 0 & 0 & 0 & 0.902255\mathrm{y1}(d)^{\frac{3}{20}} & \frac{58.15212.^{-1.26282-2.d}d(-5.+2.18719\,\mathrm{y1}(d))^{-1.+d}}{\mathrm{y1}(d)^{\frac{7}{20}}} & \frac{0.221596}{\mathrm{y1}(d)^{\frac{17}{20}}} & -6.86418\mathrm{y1}(d)^{\frac{3}{20}} & 0
\end{bmatrix}
$$

Table 6: State Space Transition Matrix

$$Aux(d) = \begin{bmatrix} 0 & 0 & 0 & 0 & 0 & 0 & 0 & 0 & 0 & 0 & 0 & 0 & 0 & 0 & 0 & 0 & 0 & 0 & 0 & \frac{-35\,y1^{\frac{3}{20}}}{42^{\frac{1}{12}}} & 0 & \frac{-3\sqrt{5}}{22^{\frac{3}{4}}\,y1^{\frac{17}{20}}} & 0 & 1 \\ -\frac{1}{10} & 0 & 0 & 0 & 0 & 0 & 0 & 0 & 0 & 0 & 0 & 0 & 0 & \frac{1}{102^{\frac{1}{3}}\,5^{\frac{2}{3}}} & \frac{32^{-\frac{20}{39}-2d}\,3^{\frac{7}{13}d}\left(-5+\frac{93^{\frac{7}{13}}\,y1}{52^{\frac{20}{39}}\,5^{\frac{1}{39}}}\right)^{-1+d}}{55^{\frac{1}{39}}\sqrt{y1}} & 0 & 0 & 0 & 0 & \frac{-3}{102^{\frac{1}{3}}\,5^{\frac{2}{3}}} & 0 & \frac{-1}{20y1} & \frac{-993^{\frac{7}{13}}}{10002^{\frac{20}{39}}\,5^{\frac{1}{39}}} & 0 \\ 0 & 0 & 0 & 0 & 0 & 0 & 0 & 0 & 0 & 0 & 0 & 0 & 0 & 0 & 0 & \frac{-93^{\frac{7}{13}}}{202^{\frac{20}{39}}\,5^{\frac{1}{39}}} & 0 & 0 & 0 & 0 & 1 & 0 & \frac{813^{\frac{1}{13}}\,y1}{2002^{\frac{1}{39}}\,5^{\frac{2}{39}}} & 0 \\ 0 & 0 & 0 & 0 & 0 & 0 & 0 & 0 & 0 & 0 & 0 & 0 & 0 & 0 & 0 & 0 & 0 & 0 & 1 & 0 & 0 & 0 & 0 & 0 \end{bmatrix}$$

Table 7: Auxiliary Initial Conditions Dimension

$$v_t = \begin{bmatrix} w_{t-2} \\ w_{t-1} \\ x_{1,t-1} \\ x_{2,t-1} \\ w_t \\ x_{1,t} \\ x_{2,t} \\ y_{1,t} \\ y_{2,t} \end{bmatrix}$$

$A(d) =$

$$\begin{bmatrix} 0 & 1. & 0 & 0 & 0 & \cdots \\ 0 & 0 & 1. & 0 & 0 & \\ 0 & 0 & 0 & 0 & 0 & \\ 0 & 0 & 0 & 0 & 0 & \\ 0 & 0 & 0 & 0 & 0 & \\ 0 & 0 & 0 & 0 & 0 & \\ -1.61688 & -1.22801 & 0 & 0.438889 & \frac{-1.689852.^{0.820513-2.d} d(-5.+2.18719\,\mathrm{y1}(d))^{-1.+d}}{\sqrt{\mathrm{y1}(d)}} & \\ -0.546798\,\mathrm{y1}(d) & 0 & 0 & 0.148424\,\mathrm{y1}(d) & 0 & \\ -0.666667\,\mathrm{y1}(d) & 0 & 0 & 0.180961\,\mathrm{y1}(d) & 1.733762.^{1.48718-2.d} d\sqrt{\mathrm{y1}(d)}(-5.+2.18719\,\mathrm{y1}(d))^{-1.+d} & \\ 1.37162 & 0 & 0 & -0.372315 & 0 & \end{bmatrix}$$

$$\begin{bmatrix} 0 & 0 & 0 & 0 & 0 \\ 0 & 0 & 0 & 0 & 0 \\ 1. & 0 & 0 & 0 & 0 \\ 0 & 1. & 0 & 0 & 0 \\ 0 & 0 & 1. & 0 & 0 \\ 0 & 0 & 0 & 0 & 0 \\ 0 & 0.333333 & \frac{5.069552.^{0.820513-2.d} d(-5.+2.18719\,\mathrm{y1}(d))^{-1.+d}}{\sqrt{\mathrm{y1}(d)}} & \frac{-0.409337}{\mathrm{y1}(d)} & -1.94504 \\ 0 & 0 & 0 & 0.546798 & -0.657775\,\mathrm{y1}(d) \\ 0 & 0 & 0 & 0.666667 & -0.801971\,\mathrm{y1}(d) \\ 0 & 0 & 0 & 0 & 1.65 \end{bmatrix}$$

Table 8: Reduced Dimension State Space Transition Matrix